Optimization of Turbine Tilt in a Wind Farm

James J. Cutler*, D. John Prymak Jr.†
Brigham Young University, Department of Mechanical Engineering, Provo, UT, 84602

Wind farms are severely affected by negative wake interactions between turbines. By optimizing the tilt angle of the turbines in a farm, wakes may be deflected away from downstream turbines, increasing the overall energy production. In this study, we will optimize the tilt angle of turbines in a wind farm to maximize energy production. We will use an analytic wake model modified to consider wake deflection from tilt, and gradient-based optimization. We will consider optimizing the tilt angle of each turbine assuming that it will remain fixed for the lifetime of the farm. We will also consider active tilt control. Preliminary results with optimization of the Princess Amalia Wind Farm show about an 11% increase in the annual energy production. Although these preliminary results only consider one wind farm we expect that considering other wind farms will still result in significant gains.

I. Introduction

As the world continues to pursue renewable energy goals, it is increasingly important to improve the efficiency of wind farms. Wind farms lose up to 15% to 20% of energy production throughout the year because of wake interference between turbines [1–4], and up to 40% for farms with closely spaced wind turbines [5]. One method that is currently used to reduce wake interference between turbines in a farm is through active control. Many studies have found that by yawing turbines, the wakes can be deflected and steered away from downstream turbines. Yawing the upstream turbines causes the energy production of these turbines to decrease, however, the reduced waking of downstream turbines can result in a net gain [6–9]. Gebraad et al. observed that with optimal yaw angles the net annual energy production (AEP) for a simple 2 by 3 wind turbine wind farm can increase by as much as 13% [10]. Gebraad et al. also observed that along with increasing annual energy production another benefit of yawing is a decrease in the loads experienced on the yawed turbines [6]. Conversely, due to the reduction in rotor swept area from yawing turbines the wake deflection may sometimes not be enough and there can be a net decrease in the energy production of the farm [3].

Yawing turbines deflects turbine wakes in the horizontal plane, and can result in significant energy gains in a wind farm. Another similar method that has not been explored as thoroughly is wake deflection through turbine tilt. Just as yaw control can be used to deflect downstream wakes in the horizontal plane, tilt control can be used to deflect wakes up and down. The benefits of tilting turbines are not as easy to research, mainly because turbines do not yet have active tilt capabilities making it difficult to verify results in a real wind farm. However, there has been some research done exploring turbine tilt. An early study by Guntur et al. found that similar to yaw, tilt in a wind turbine can effectively deflect the wake. However, they suggest active tilt control appears to be rather impractical because the amount of tilt needed for significant gains in power production could run the blades into the tower [11].

More recent studies are more favorable and indicate that there may be significant benefits to wake deflection from turbine tilt. Annoni et al. analyzed possible increases in the energy production due to active tilt control in a row of two of NREL's 5-MW reference turbines. Using the large-eddy simulation tool SOWFA(Simulator fOr Wind Farm Applications) [12], they found that when the turbines were placed 7 rotor diameters apart a positive tilt of about 25 ° in the front turbine deflected the wake enough for an 8.3% net increase in energy production [13]. Such results however do not attempt to test all possible tilt angles to find the optimal tilt angles for highest gains in power production because they are limited by an expensive simulation. Thus, they are limited by computational expense to only test some scenarios.

This research will go beyond tilt control in a few turbines in a row with one wind direction, and explore tilt angle and active tilt control optimization for a full wind farm. By using an analytic wake model, we will be able to quickly model an entire farm, and study the benefits of wake deflection from turbine tilt for a wind farm layout and its associated wind distribution. We will consider optimizing the tilt angles that will remain fixed throughout the lifetime of the farm. With current technology, these findings will be able to be immediately applied to wind farm designs. We will also consider control of turbine tilt. A tilt mechanism would also be expensive and complicated to engineer, as well

*Undergraduate Research Assistant
†Master's Candidate

as increase turbine capital costs. However, this study will be an early step in determining if the benefits of active tilt control are worth the difficulty of implementing it in real wind farms.

II. Methodology

A. Wake Model

In this section we discuss the wake model used to predict wake interactions in order to calculate AEP. We used a modified version of the Bastankhah model (shown in Eq. 1), an analytic Gaussian wake model [14]. The original formulation of the Bastankhah model does not accurately model the near wake of a wind turbine, but it can accurately model the far wake. In this paper we will only consider wind farms with turbines spaced relatively far apart (greater than 5 rotor diameters) such that only far wake interactions are relevant. In their paper, Bastankhah et al. state that the model can be used to predict wake deflection from turbine tilt in a similar manner to how they predict deflection from yaw. Thus, we modified their equations to consider turbine tilt in the wind speed deficit and wake deflection calculations [14].

$$\frac{\triangle\overline{u}}{\overline{u}_\infty} = \left(1 - \sqrt{1 - \frac{C_T\cos(\gamma)}{8(\sigma_y\sigma_z/d^2)}}\right)\exp\left[-0.5\left(\frac{y-\delta}{\sigma_y}\right)^2\right]\exp\left[-0.5\left(\frac{z-z_h}{\sigma_z}\right)^2\right] \tag{1}$$

This equation includes the thrust coefficient (C_T), rotor diameter (d), turbine tilt angle (γ), the distance between the point of interest and the wake center in the cross-stream horizontal ($y-\delta$) and vertical ($z-z_h$) directions, and the wake widths in the cross-stream horizontal and vertical directions (σ_y and σ_z).

The wake widths, σ_y and σ_z, are defined in Eqs. 2 and 3.

$$\frac{\sigma_y}{d} = k_y\frac{x-x_0}{d} + \frac{1}{\sqrt{8}} \tag{2}$$

$$\frac{\sigma_z}{d} = k_z\frac{x-x_0}{d} + \frac{\cos(\gamma)}{\sqrt{8}} \tag{3}$$

In these equations, x is the downstream distance from the wind turbine creating the wake, d is the rotor diameter of the turbine, x_0 is the length of the wake potential core, and k_y and k_z are constants with the values based on turbulence intensity as defined in Eq. 4 [15]. We assumed a turbulence intensity of 0.075.

$$k = 0.3837I + 0.003678 \tag{4}$$

To know where the far wake can begin to be defined the length of the potential core is first calculated. The length of the potential core is defined by the following function where $\alpha = 2.32$ and $\beta = 0.154$.

$$\frac{x_0}{d} = \frac{\cos(\gamma)(1+\sqrt{1-C_T})}{\sqrt{2}(\alpha I + \beta(1-\sqrt{1-C_T}))} \tag{5}$$

Interacting wakes are defined with linear superposition, as described by Niayifar et al. [15].

To make sure the tilt deflection in our analytic Gaussian wake model is working as expected, we plotted the velocity field for a few tilt angles. Figure 1 shows the velocity field behind a turbine tilted at 5°, 15°, and 30°. As the tilt increases from 5° to 30°, the wake deflects more and more towards the ground as expected. These results are similar to the results of Annoni et al. who used SOWFA to model their wake deflection [13].

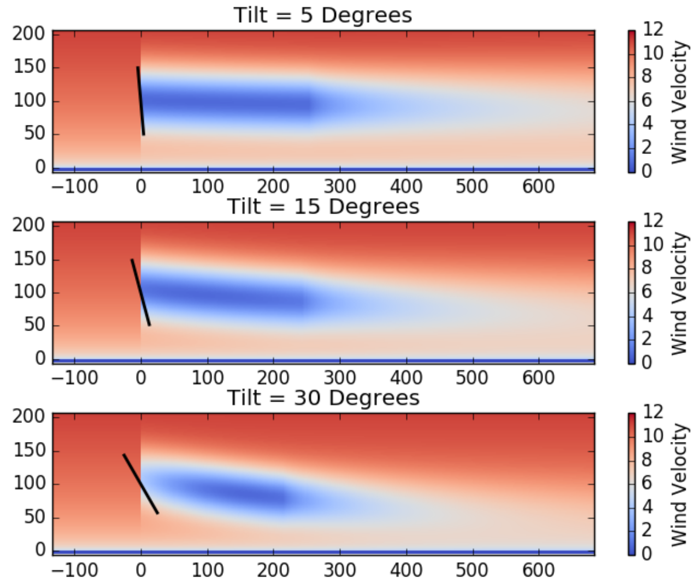

Figure 1 Visualization of the wake of a single turbine being tilted 5 °, 15 °, and 30 ° using the analytic Gaussian wake model.

Because of increased turbulence close to the ground, we expect that a wind turbine wake near the ground will dissipate more quickly than one higher up [16]. This is similar to propeller wake ground interactions which have been studied in past experiments and models [17]. Our current wake model does not account for ground effects, but in the conference version of this paper we will include the turbulence intensity as a function of height, similar to what was proposed by Cheung et al. [18].

B. Wind Farm Power

In this section we discuss how we calculate the wind farm power. The power produced by a single turbine is expressed in Eq. 6.

$$P_i = \begin{cases} 0 & V_{\text{avg}} < V_{\text{cut-in}} \\ \frac{1}{2}\rho A_{\text{eff}}(V_{\text{avg}})^3 C_P & V_{\text{cut-in}} \leq V_{\text{avg}} < V_{\text{rated}} \\ \frac{1}{2}\rho A_{\text{eff}}(V_{\text{rated}})^3 C_P & V_{\text{rated}} \leq V_{\text{avg}} < V_{\text{cut-out}} \\ 0 & V_{\text{avg}} \geq V_{\text{cut-out}} \end{cases} \tag{6}$$

Where $\rho = 1.225$ and represents the density of air, A is the rotor swept area (our preliminary results used a rotor diameter of 100 meters), C_P is the turbine power coefficient (our preliminary results used an idealized C_P of 0.592), $V_{\text{cut-in}} = 3.5$ m/s and is the cut-in wind speed, $V_{\text{cut-out}} = 25$ m/s and is the cut-out wind speed, $V_{\text{rated}} = 14$ m/s and is the rated wind speed, and V_{avg} is the effective wind speed across the rotor hub [15].

The effective velocity across the rotor hub, V_{avg}, is calculated as an average of velocities at 20 points dispersed within the rotor swept area of a turbine. The velocity measured at each one of the 20 points is calculated by taking the free-stream velocity at the height of the point of interest minus the velocity deficit in Eq. 1. The free stream velocity is calculated as a function of height using an exponential wind power curve with a shear exponent of 0.15.

When a turbine is tilted it will produce less power due to the reduction of the projected rotor swept area. To account for this reduction, the power of each turbine is calculated by multiplying the rotor swept area by $\cos(\gamma)^{1.88}$[13].

$$A_{\text{eff}} = A \cos(\gamma)^{1.88} \tag{7}$$

Based on the direction that a turbine is tilted, the wakes of upstream turbines can be deflected either towards the top or bottom of the downstream turbines. Lower wind speeds at lower heights suggest that the bottom of the rotor swept area is more beneficial to deflect the upstream wakes into. Leaving the upper portions of the rotor swept area exposed to the free stream velocities therefore allowing the turbine to experience a higher average wind speed and consequently produce more power.

C. Optimization

In order to find the optimal turbine position and tilt angle for maximum AEP of a wind farm, we will use a sparse non-linear optimization algorithm called SNOPT [19]. We will use finite-differencing gradients for each optimization scenario, and use at least 50 random starting points to sufficiently search the function space. To avoid having too many design variables and isolate the effects of turbine tilt, hub-height, and turbine position we will be performing multiple test cases and comparing the maximum AEP. The percent difference from the baseline performance of the Princess Amalia wind farm as calculated by our model will be reported.

The following test cases will be used to maximize AEP:

- Test case 1: Adjust fixed turbine tilt angles with turbines fixed to Amalia wind farm turbine positions
- Test case 2: Adjust fixed turbine hub-heights with turbines fixed to Amalia wind farm turbine positions
- Test case 3: Active tilt control with turbines fixed to Amalia wind farm turbine positions
- Test case 4: Adjust turbine positions with tilt fixed to optimal tilt layout from test case 1.
- Test case 5: Adjust turbine positions with hub-heights fixed to optimal hub-height layout from test case 1.

The design variables for test cases 1 and 3 will include the tilt angle of each turbine (γ) and test case 2 will include the hub-height of each turbine (h). For test cases 1 and 2 the design variables will be the same for every wind direction, whereas for active tilt control in test case 3 the tilt angle can vary with every wind direction. These three test cases all have the positions of the turbines fixed to the layout of the Princess Amalia Wind Farm. Test cases 1 and 3 are defined in Eq. 8 and test case 2 is defined by Eq. 9. Changing the hub-heights of the turbines in a wind farm can deflect wakes away from downstream turbines similar to tilt. Therefore, the AEP of these optimization scenarios can measure the possible benefits of fixed tilt angles and active tilt control over fixed hub-heights. If the active tilt control increases the AEP significantly greater than fixed tilt angles and fixed hub-heights then it suggests developing the ability to tilt a wind turbine could prove beneficial.

The tilt angles will be constrained to a maximum of 30 ° in the negative and positive direction. A tilt angle of negative 30 ° may be extreme, however as stated earlier this study is to explore the benefits of tilt optimization with the assumption that such a tilt angle could be possible. Considering the rotor diameter of each turbine to be 100 meters the hub-height of each turbine will be constrained to a minimum of 70 meters and a maximum of 150 meters. These constraints are defined in Eq. 8 and Eq. 9.

$$\begin{aligned}
&\text{maximize} && \text{AEP} && \\
&\text{w.r.t.} && \gamma_i \ (i = 1, \ldots, \text{nTurbines}) && \text{(fixed tilt angle)} \\
& && \gamma_{i,j} \ (i = 1, \ldots, \text{nTurbines},\ j = 1, \ldots, \text{nDirections}) && \text{(active tilt control)} \\
&\text{subject to} && -30^\circ \le \gamma_i \le 30^\circ &&
\end{aligned} \tag{8}$$

$$\begin{aligned}
&\text{maximize} && \text{AEP} && \\
&\text{w.r.t.} && h_i \ (i = 1, \ldots, \text{nTurbines}) && \text{(fixed variable hub-heights)} \\
&\text{subject to} && 70 \text{ meters} \le \gamma_i \le 150 \text{ meters} &&
\end{aligned} \tag{9}$$

The optimal positions for a wind farm using variable tilt is likely very different from optimal positions not considering tilt (i.e. current layout of Princess Amalia wind farm). The test cases 4 and 5 will allow the optimizer to vary the positions of each turbine. This is a more realistic scenario as with the additional consideration of tilt it is unlikely that this capability will be added to an existing wind farm. The optimal fixed tilt angles and fixed hub-heights that result in maximum AEP for the first two test cases will then be fixed and the position of each turbine will be the design variables for test cases 4 and 5. The design variables and constraints for test cases 4 and 5 are defined in Eq. 10. These scenarios will allow the AEP to potentially increase more as the position of each turbine is no longer constrained to the layout of the Princess Amalia Wind Farm. Instead, each turbine will be constrained to be within the boundary defined by a convex hull of the existing Princess Amalia Wind Farm layout, and the distance between each turbine must be greater than five rotor diameters.

$$
\begin{aligned}
\text{maximize} \quad & \text{AEP} \\
\text{w.r.t.} \quad & x_i, y_i \ (i = 1, \ldots, \text{nTurbines}) \qquad \text{(fixed optimum tilt angles)} \\
& x_i, y_i \ (i = 1, \ldots, \text{nTurbines}) \qquad \text{(fixed optimum hub-heights)} \\
\text{subject to} \quad & S_{i,j} \geq 500 \text{ meters} \\
& C_{x,low} \leq x_i \leq C_{x,high} \\
& C_{y,low} \leq y_i \leq C_{y,high}
\end{aligned}
\tag{10}
$$

In Eq. 10, C_x and C_y represent the wind farm boundaries with respect to the x and y coordinates of each turbine. $S_{i,j}$ is the spacing between pairs of turbines i and j.

1. Scaling

In order to improve the effectiveness of the test cases we scaled some of the variables. The AEP is calculated initially in watts, however this is difficult to optimize when AEP for these test cases ranges from around 200 GWh to 600 GWh. Therefore the AEP value that is passed through SNOPT is divided by 10^9 in order to be in units of GWh. The constraint values used in test cases three and four for defining the distance between turbines and the distance from turbines to wind farm boundaries range from around 100 to 1000. Therefore the constraint values are divided by 1000. Before adding this scaling the optimizations ran quickly and converged to small values for AEP.

2. Wind Rose Simplification for Optimizations

The initial optimizations were run with the original wind rose data from the Amalia wind farm defined in Fig. 2. However, for the first optimization scenario this required up to 50,000 function calls and 10 hours to optimize 10 random starting points. With constraints to time, a simplified wind rose of 15 wind directions was derived based on the original wind rose data of 60 wind directions. The simplified wind rose is defined in Fig. 3. This simplification allowed for the first optimization scenario to finish optimizing 50 random samples in under 5 hours.

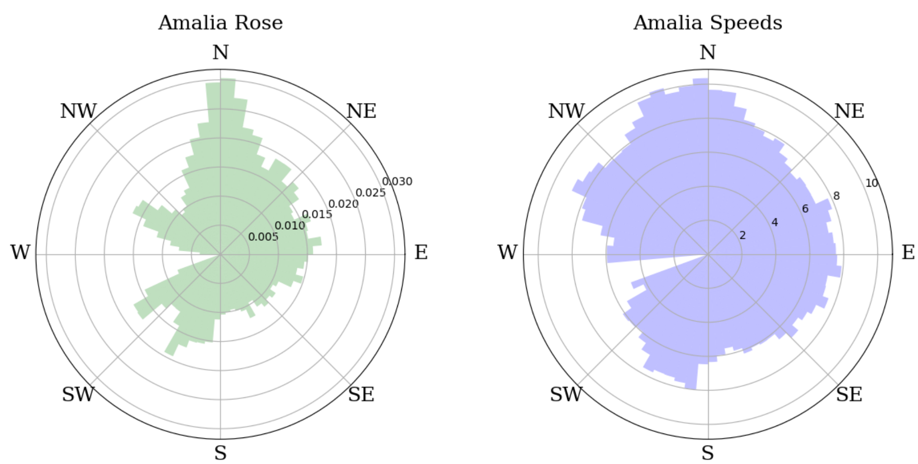

Figure 2 Wind speeds and associated frequencies and directions for the Princess Amalia Wind Farm.

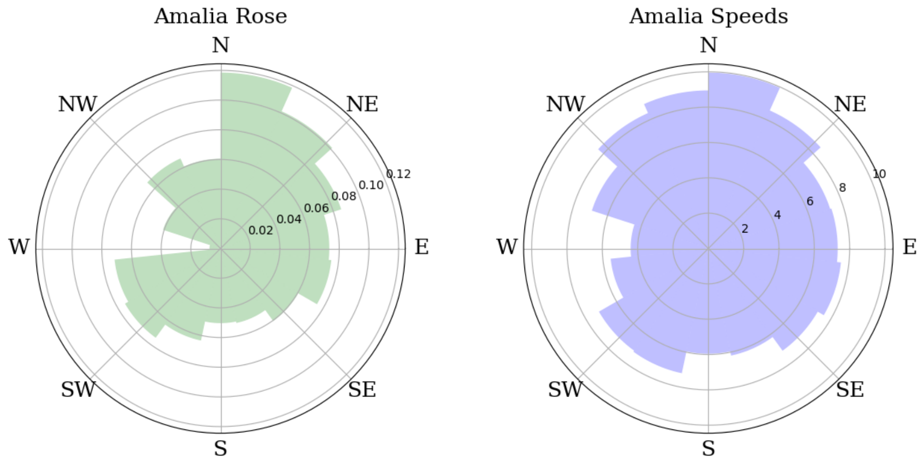

Figure 3 Simplified wind speeds and associated frequencies and directions for the Princess Amalia Wind Farm.

III. Results and Discussion

A. Fixed Princess Amalia Wind Farm Layout

The first three test cases were all done with the turbine positions fixed to the layout of the Princess Amalia Wind Farm. This enables a valid comparison of the optimized AEP from active tilt control, fixed variable tilt angles, and fixed variable hub-heights. The results are listed in Table 1 where the percent gain is based off the AEP of a fixed Amalia Wind Farm layout(339.997GWh) with all tilt angles fixed at 3° and all hub-heights fixed at 150 meters. Based on these results we can conclude that the three different design variables all can significantly increase the AEP of the wind farm by at least 6.9%. However, having fixed tilt as opposed to fixed variable height did not yield a noticeable difference between each other. We expected something like this as the positions were not optimized for these specific design variables.

	Annual Energy Production(GWh)	Percent Gain
Fixed Tilt	366.7	7.3
Variable Height	365.3	6.9
Active Tilt Control	384.1	11.5

Table 1 Optimized AEP based on fixed tilt angles, variable hub-heights, and active tilt control

Figure 4 displays that major tilt angles tend to form in lines of nearby turbines rather than in clusters of nearby turbines. The more neutral tilt angles tend to appear around the lines of turbines with major tilt angles. This suggests that when designing the layout of a wind farm with tilt capabilities it will increase AEP best by creating rows of large tilt angles in the turbines and nearby rows of more neutral tilt angles. The rows of majorly tilted turbines allows for the more neutrally tilted turbines to experience a higher average wind speed in their rotor swept areas.

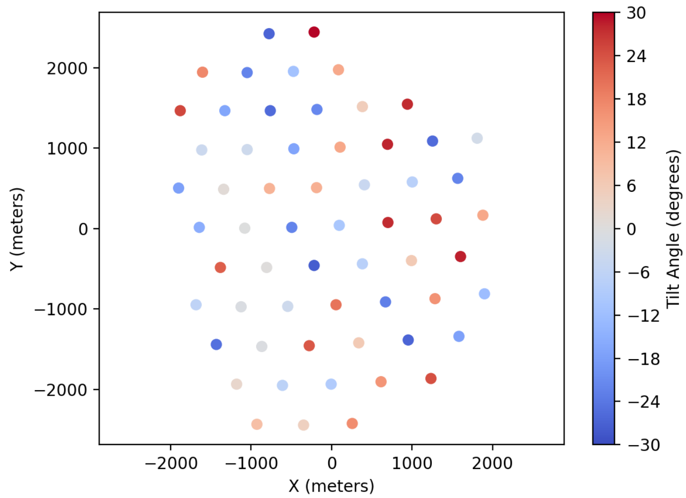

Figure 4 Wind turbine locations in the Amalia wind farm with associated values for tilt angles that produced the max AEP.

Figure 5 has some similar patterns with some rows of shorter hub-heights, however there are few rows with tall hub-heights. Instead, there are gradients in rows of turbines that start short and increase in hub-height across the row. Downstream wind turbines can be exposed to higher wind speeds by rows of upstream turbines whose hub-heights gradually increase or decrease.

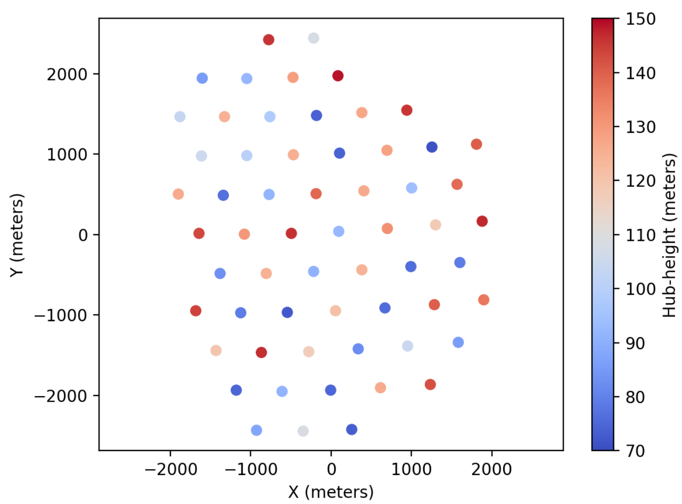

Figure 5 Wind turbine locations in the Amalia wind farm with associated values for hub-heights that produced the max AEP.

B. Fixed Tilt Angle and Hub-height

In test cases 4 and 5 the optimizer recreates the optimal tilt angles and hub-heights from previous cases and sets the design variables as the positions of each turbine. In figure 6 and 7, the optimal positions for both the hub-height and tilt optimization sample runs are displayed. The AEP values for these two test cases are found in Table 2.

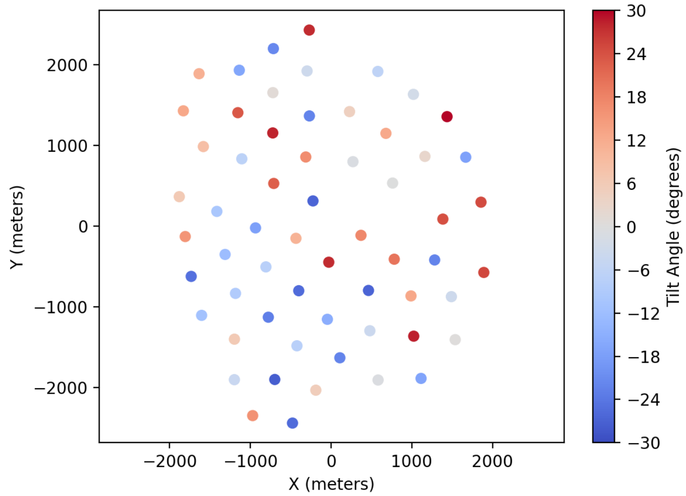

Figure 6 Wind turbine locations within the boundaries of the Amalia Wind Farm with the optimal tilt angles from test case 1.

Interestingly, optimizing the turbine positions rearranged the major tilt values to cluster slightly in the center and then branch out in different directions, forming clusters of more neutral tilt angles between the branches of major tilt angles. However, the spacing and shape of the overall wind farm does not differ significantly from the Amalia Wind Farm layout.

This change in tilt patterns allowed for the AEP to increase from a 7.3% gain to a 15.8% gain. The 15.8% gain is a more reasonable metric of how beneficial the capability of tilt in a wind farm can be than the 7.3% gain because tilt cannot be implemented in existing wind farms.

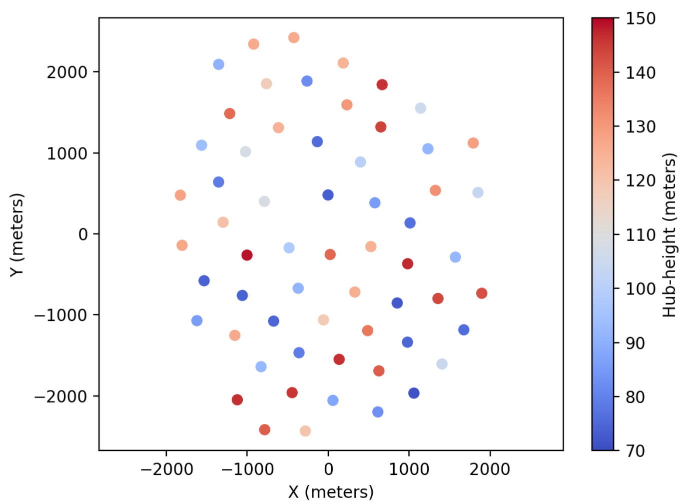

Figure 7 Wind turbine locations within the boundaries of the Amalia Wind Farm with the optimal hub-heights from test case 2.

Optimizing the position of the turbines with the optimal heights from test case 2 resulted in the hub-heights generally being tallest down south and shortest up north. This pattern matches the distribution of the wind rose in Fig. 3 where the faster wind comes more from the north during the year. This allows the wakes of the shorter hub-heights to not interfere with the rotor swept areas of the taller downstream hub-heights. Although the fixed variable height optimization has a smaller gain in AEP than the fixed variable tilt, a gain of 10% is still noteworthy. However, in designing a new wind farm, creating turbines that can be built at a fixed tilt angle could be more cost effective as they can increase the AEP by as much 5% more than using wind turbines with differing hub-heights.

	Annual Energy Production(GWh)	Percent Gain
Fixed Variable Tilt	403.6	15.8
Fixed Variable Height	378.2	10.1

Table 2 Optimized AEP based on adjusting the positions of turbines that have fixed tilt angles and fixed hub-heights.

It is likely that as turbine density is increased the benefits of using tilt will become more stark as compared to hub height variance. For fixed variable tilt there was an increase of 15% over the Princess Amalia baseline AEP. This is great performance as we know that 15% - 20% of efficiency is lost due to wind wake interactions, this method may be making a significant impact on this[10].

IV. Conclusion and Continued Development

The scenario in question for this project was can tilt control effectively increase the AEP of a wind farm. To better understand tilt controls significance we compared it to hub height control optimization. Based on the results of our test cases we can confidently say that tilt with optimized positions outperforms hub height with optimized positions. The current wind farm in question may not have the turbine density needed to see the largest benefits of tilt implementation, however we saw improvements in efficiency nonetheless. We know that wake interactions can account for a 15%-20% loss of efficiency and up to 40% in closely spaced turbine wind farms like the Princess Amalia wind farm. With an increase of 15% tilt optimization is very validating. Our results show that implementing tilt may help reduce the 40% efficiency loss of closely spaced wind farms.

A more robust model will need to be built such that tilt and position can be simultaneously optimized. We can expect a higher percent gain as the wind farm is able to position the associated tilts with more accuracy in one optimization routine. To create a more accurate wake model we will include the turbulence as a function of height. A major benefit of vertical wake deflection is being able to dissipate turbine wakes faster with ground effects. A turbulence distribution will approximate this phenomenon. To validate the accuracy of the model used it will need to be compared to data from SOWFA simulations. SOWFA is a high-fidelity tool for evaluating wind plant control[20].

Aside from fixed tilt optimization, active tilt control could have great benefits as it can adjust the tilt angles of each turbine for every wind direction, whereas fixed tilt optimization finds an optimal fixed angle for all wind directions. Further investigation will surely need to be done on active tilt control, but this will not be feasible without providing analytical gradients to speed up the optimization. However, active tilt control may be harder to justify as the cost of developing and implementing this function may exceed the benefits.

Overall, the successful implementation of tilt control and validation of its benefits could lead to the reduction in real estate costs associated with the need to space turbines farther apart. By allowing the wake interactions to be minimized, turbines can be placed closer together without significant power production losses. Therefore a further cost analysis on the possibility of building a tilt function in wind turbines and the added AEP could further explore the possibilities of tilt optimization.

For our final conference paper, we will include the several additions and improvements to our current state as stated above. When the model is improved and validated, we will optimize the tilt angle of turbines for several wind farm scenarios. We will consider several wind farm layouts, turbine spacing's, and wind distributions to understand the benefits of tilt optimization in different circumstances. As mentioned before, we will consider fixed tilt angle optimization, as well as active tilt control.

References

[1] Barthelmie, R. J., Frandsen, S. T., Nielsen, M., Pryor, S., Rethore, P.-E., and Jørgensen, H. E., "Modelling and measurements of power losses and turbulence intensity in wind turbine wakes at Middelgrunden offshore wind farm," *Wind Energy*, Vol. 10, No. 6, 2007, pp. 517–528.

[2] Barthelmie, R. J., Hansen, K., Frandsen, S. T., Rathmann, O., Schepers, J., Schlez, W., Phillips, J., Rados, K., Zervos, A., Politis, E., et al., "Modelling and measuring flow and wind turbine wakes in large wind farms offshore," *Wind Energy*, Vol. 12, No. 5, 2009, pp. 431–444.

[3] Barthelmie, R. J., and Jensen, L., "Evaluation of wind farm efficiency and wind turbine wakes at the Nysted offshore wind farm," *Wind Energy*, Vol. 13, No. 6, 2010, pp. 573–586.

[4] Briggs, K., "Navigating the complexities of wake losses," *Norik American Windpower*, Vol. 10, 2013.

[5] Stanley, A. P. J., Ning, A., and Dykes, K., "Optimization of Turbine Design in Wind Farms with Multiple Hub Heights, Using Exact Analytic Gradients and Structural Constraints," *Wind Energy*, Vol. 22, No. 5, 2019, pp. 605–619. https://doi.org/10.1002/we.2310.

[6] Gebraad, P. M., Teeuwisse, F., van Wingerden, J.-W., Fleming, P. A., Ruben, S. D., Marden, J. R., and Pao, L. Y., "A data-driven model for wind plant power optimization by yaw control," *2014 American Control Conference*, IEEE, 2014, pp. 3128–3134.

[7] Fleming, P. A., Ning, A., Gebraad, P. M., and Dykes, K., "Wind plant system engineering through optimization of layout and yaw control," *Wind Energy*, Vol. 19, No. 2, 2016, pp. 329–344.

[8] Fleming, P., Annoni, J., Shah, J. J., Wang, L., Ananthan, S., Zhang, Z., Hutchings, K., Wang, P., Chen, W., and Chen, L., "Field test of wake steering at an offshore wind farm," *Wind Energy Science*, Vol. 2, No. 1, 2017, pp. 229–239.

[9] Gebraad, P., Thomas, J. J., Ning, A., Fleming, P., and Dykes, K., "Maximization of the Annual Energy Production of Wind Power Plants by Optimization of Layout and Yaw-Based Wake Control," *Wind Energy*, Vol. 20, No. 1, 2017, pp. 97–107. https://doi.org/10.1002/we.1993.

[10] Gebraad, P., Teeuwisse, F., Van Wingerden, J., Fleming, P. A., Ruben, S., Marden, J., and Pao, L., "Wind plant power optimization through yaw control using a parametric model for wake effects—a CFD simulation study," *Wind Energy*, Vol. 19, No. 1, 2016, pp. 95–114.

[11] Guntur, S., Troldborg, N., and Gaunaa, M., "Application of engineering models to predict wake deflection due to a tilted wind turbine," *EWEA 2012-European Wind Energy Conference & Exhibition*, European Wind Energy Association (EWEA), 2012.

[12] Churchfield, M., Lee, S., and Moriarty, P., "Overview of the simulator for wind farm application (SOWFA)," *National Renewable Energy Laboratory*, 2012.

[13] Annoni, J., Scholbrock, A., Churchfield, M., and Fleming, P., "Evaluating tilt for wind plants," *2017 American Control Conference (ACC)*, IEEE, 2017, pp. 717–722.

[14] Bastankhah, M., and Porté-Agel, F., "Experimental and theoretical study of wind turbine wakes in yawed conditions," *Journal of Fluid Mechanics*, Vol. 806, 2016, pp. 506–541.

[15] Niayifar, A., and Porté-Agel, F., "Analytical modeling of wind farms: A new approach for power prediction," *Energies*, Vol. 9, No. 9, 2016, p. 741.

[16] Hyvärinen, A., and Segalini, A., "Qualitative analysis of wind-turbine wakes over hilly terrain," *Journal of Physics: Conference Series*, Vol. 854, IOP Publishing, 2017, p. 012023.

[17] Puel, F., and de Saint Victor, X., "Interaction of wake vortices with the ground," *Aerospace science and technology*, Vol. 4, No. 4, 2000, pp. 239–247.

[18] Cheung, L., Premasuthan, S., Davoust, S., and von Terzi, D., "A simple model for the turbulence intensity distribution in atmospheric boundary layers," *Journal of Physics: Conference Series*, Vol. 753, IOP Publishing, 2016, p. 032008.

[19] Gill, P. E., Murray, W., and Saunders, M. A., "SNOPT: An SQP algorithm for large-scale constrained optimization," *SIAM review*, Vol. 47, No. 1, 2005, pp. 99–131.

[20] Fleming, P., Gebraad, P., van Wingerden, J.-W., Lee, S., Churchfield, M., Scholbrock, A., Michalakes, J., Johnson, K., and Moriarty, P., "SOWFA super-controller: A high-fidelity tool for evaluating wind plant control approaches," Tech. rep., National Renewable Energy Lab.(NREL), Golden, CO (United States), 2013.